heritage

MDPI

Article

Characterization of Natural Stone from the Archaeological Site of Pella, Macedonia, Northern Greece

Panayotis K. Spathis [1,*], Maria Mavrommati [1], Eirini Gkrava [1], Vasilios Tsiridis [2], Sotiris P. Evgenidis [1], Ioannis Karapanagiotis [3], Vasilios Melfos [4] and Thodoris D. Karapantsios [1]

1 Department of Chemistry, Aristotle University of Thessaloniki, GR-54124 Thessaloniki, Greece; mariaparanaue@gmail.com (M.M.); irene_xanthi@yahoo.gr (E.G.); sevgenid@chem.auth.gr (S.P.E.); karapant@chem.auth.gr (T.D.K.)
2 Department of Civil Engineering, Aristotle University of Thessaloniki, GR-54124 Thessaloniki, Greece; tsiridis@civil.auth.gr
3 Department of Management and Conservation of Ecclesiastical Cultural Heritage Objects, University Ecclesiastical Academy of Thessaloniki, GR-54250 Thessaloniki, Greece; y.karapanagiotis@aeath.gr
4 Department of Geology, Aristotle University of Thessaloniki, GR-54124 Thessaloniki, Greece; melfosv@geo.auth.gr
* Correspondence: spathis@chem.auth.gr

Abstract: The goal of the study was to characterize the limestone that was used extensively in the ancient city of Pella (Macedonia, Greece), the birthplace of Alexander the Great. An on-site examination of the building material was carried out to record the types of damage and to select sampling areas. A variation in the nature of the stone and the degree of deterioration, even between the stones that comprise a specific monument structure, was observed, with water absorption and biological colonization being the main factors resulting in the deterioration of the stone. A comprehensive microanalysis and testing scheme was conducted to fully characterize the mineralogical, chemical, mechanical and thermal properties of the stones collected from various areas of the archaeological site. Optical microscopy, XRD and SEM–EDX were used to investigate the chemical composition and the structure of the stone samples. Finally, other properties, such as porosity, specific gravity and water absorption, were measured. Surface alterations, material degradation and biological deterioration were observed in most samples. The results obtained using XRD showed that the dominant mineral phase of the limestone is calcite, with quartz and clay minerals also detected in traces. The microscopic examination of the samples showed that the main natural stone at the archaeological site is a marly limestone. Thermographical measurements showed that the decay of the stones due to ambient temperature variation and corresponding contraction/expansion phenomena may be relatively limited, as the stone exhibited a low thermal diffusivity. Moreover, high porosity values (12.06–21.09%) and low compressive strength (11.3–27.7 MPa) were recorded, indicating the vulnerability of the stone and the need to take conservation measures.

Keywords: Pella; limestone; stone characterization; microscopic examination

Citation: Spathis, P.K.; Mavrommati, M.; Gkrava, E.; Tsiridis, V.; Evgenidis, S.P.; Karapanagiotis, I.; Melfos, V.; Karapantsios, T.D. Characterization of Natural Stone from the Archaeological Site of Pella, Macedonia, Northern Greece. *Heritage* **2021**, *4*, 4665–4677. https://doi.org/10.3390/heritage4040257

Academic Editors: Elisabetta Zendri, Ekaterini Delegou, Michael Turner and Antonia Moropoulou

Received: 31 August 2021
Accepted: 10 December 2021
Published: 15 December 2021

1. Introduction

The characterization of materials in the artefacts and monuments of cultural heritage is very important because it offers valuable information to archaeology and to conservation science and practice. The most common building material found in the archaeological sites in Greece are limestone, conglomerate, sandstone, travertine and marble [1]. Marly limestone is the main construction material in the archaeological site of Pella, the capital of ancient Macedonia and the birthplace of Alexander the Great [2,3]. The rich findings, which came to light after excavations, revealed the wealth and prosperity of the city, which thrived from the second half of the 4th century to the 2nd century BC. Remains of buildings, such as the temples of the goddesses Kyveli and Venus, and luxury mosaic floors and columns

are among the important findings that should be protected and conserved. Moreover, the Palace of Pella, built with blocks of limestone, has been discovered in the northern part of the city.

The marly limestone, which was used in the past as the main building material in the city of Pella, is the most common local rock [4] and has poor durability. The poor mechanical properties of the limestone in Pella were known in antiquity. For this reason, the stone was probably covered by a layer of material that played the role of a protective barrier [2]. Biological colonization observed particularly in the areas of fine grains [5] is another important factor that contributes to the poor state of preservation of the limestone. Moreover, the archeological site of Pella is located in a rural area and is exposed to the local atmospheric conditions. High levels of humidity and strong winds are recorded for long periods, particularly during the winter months. Frequent and heavy rainfall increases the soil water content, thus promoting the growth of microorganisms. Water that originates from humidity or rain causes the decay of natural stone through mechanical stresses developed by freezing/thawing cycles [6,7]. In the summer, intense sunshine increases the temperature at the stone surface, resulting in temperature gradients along the stone's cross section. The decay of limestone caused by the effects of the atmospheric conditions was extensively studied in the past [8–10]. The physicomechanical characterization of the stone of the archaeological site of Pella was carried out in several studies, which employed optical microscopy and reported petrographic results [2,3,5]. Liali et al. [2] studied the state of the building materials of the Monumental Propylon and Building I of the Palace of Pella and showed that up to 60% of the stones examined were highly deteriorated, presenting cracks, exfoliation, detachments, discontinuities, biological growths and, in some cases, complete disintegration. Interestingly, the authors suggested that up to 3717 stones need conservation, while 110 stones should be replaced. In the same study, the compressive strength of the stone showed a relatively high variation (20–60 MPa), indicating the unstable quality of the material. Relatively lower compressive strength was reported by Papayianni et al. [3], ranging from 30 to 45 MPa for healthy stone samples and from 11.5 to 15.0 MPa for heavily deteriorated stone samples. Therefore, the overall state of the stone leads to an urgent need for conservation and restoration measures. The majority of the adopted measures include the protection of stone remnants with repair mortars, cleaning, and consolidation of stones with calcium hydroxide suspensions [2].

In this study, several analytical techniques were applied to evaluate the petrographic, physicochemical, physicomechanical and thermographical properties and the state of preservation of stone samples collected from the archeological site of Pella. The results will be used in the future to develop an appropriate conservation plan of the stone. The petrographic, isotopic and physicochemical characteristics were evaluated using stereomicroscopy, polarized light microscopy, mass spectrometry and scanning electron microscopy coupled with energy-dispersive X-ray spectroscopy (SEM–EDS). Moreover, porosity, specific gravity, water absorption, compressive strength and capillary absorption were measured. For the thermographical study, both the thermal conductivity and diffusivity of the stone samples were measured. Similar analytical schemes have been used in recent studies, offering important results about the characteristics and the properties of natural stones found in monuments of cultural heritage [11,12].

2. Materials and Methods

An on-site observation of the condition of the natural stone in the archaeological site of Pella was initially conducted and the sampling areas were selected. A general view of the archaeological site of Pella is shown in Figure 1a, while the locations of the sampling points are shown in Figure 1b. A series of up to 22 limestone samples were collected from 7 locations, including the House of Dionysus, the House of the Abduction of Helen, the House of "Koniamaton" and the public bath.

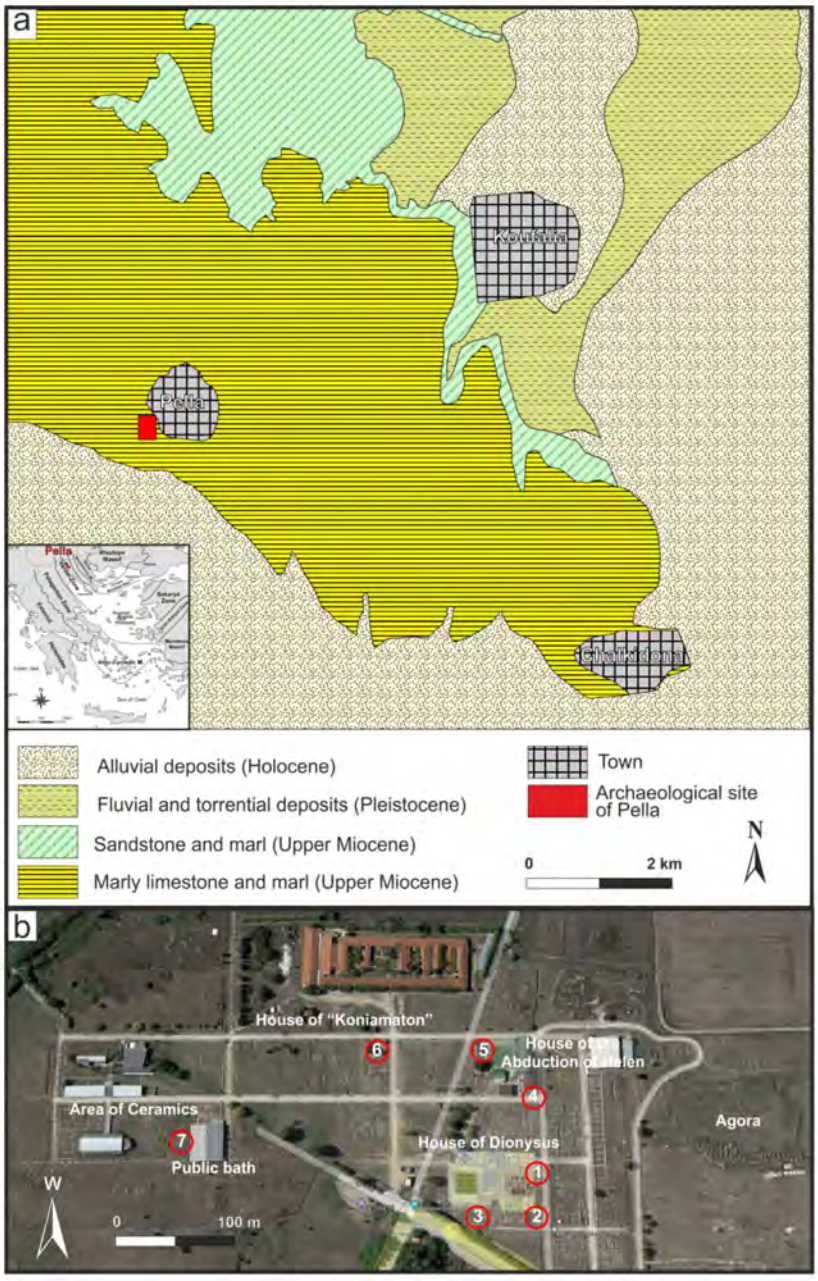

Figure 1. Geological map of the broader area of Pella, after Xydas and Efstratides [4] (**a**) and the locations of the sampling points (**b**).

Sampling areas were selected according to macroscopic observation of the stones. Special care was taken to obtain representative stone pieces without affecting the structure of the archaeological monuments. Hence, samples were practically detached pieces that belonged to areas of low aesthetic and archaeological value. Curved or architectural parts were not selected for sampling. It is noted that due to the large area of the archaeological site and the large variety of the macroscopic characteristics of the stones (even within stones at a specific area), stone samples from the Palace of Pella area were not included in this study. Photographs of samples, which were investigated herein, are provided in Figure 2. The analyses that required a small sample size (e.g., microscopy, SEM–EDS) were performed for one sample from each of the seven locations. Physicomechanical measurements require large samples and, therefore, they were not carried out for all sampling locations. The analyses per sample that were performed herein are summarized in Table 1.

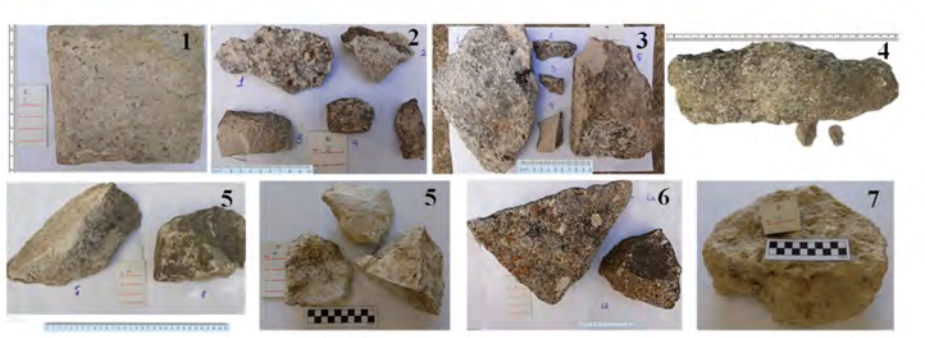

Figure 2. Stone samples collected from the seven sampling locations.

Table 1. Analyses performed on the stones collected from each of the seven sampling locations.

Analysis/Technique	Sampling Locations						
	1	**2**	**3**	**4**	**5**	**6**	**7**
Stereomicroscopy	√	√	√	√	√	√	√
Isotopic					√		
Polarizing light microscopy				√	√	√	
SEM–EDS	√	√	√	√	√	√	√
XRD		√	√	√	√	√	√
RILEM CPC 11.3		√	√	√	√		√
Capillary water absorption	√	√	√	√	√	√	
Compressive strength	√			√		√	√
Thermographical	√	√					

A microstructure observation of the stone samples was performed with stereoscope (Leica Wild M10) assisted by image analysis (ProgRes) and polarizing light microscopy by thin sections (Leitz Laborlux N POLS). Isotopic analysis was performed by the Iso-Analytical Laboratory, UK, using a continuous flow isotope ratio mass spectrometer (CF-IRMS). The O- and C-isotope ratios were referred to the standard VPDB (Vienna Pee Dee Belemnite). An X-ray diffraction (Bruker D 2 PHASER) analysis was carried out in powder samples with a diameter of granules <75 μm. The Crystallography Open Database was used for the interpretation of the results. Scanning electron microscopy (SEM) equipped with energy-dispersive X-rays (EDS) was employed to carry out elemental analysis (JEOL JMS-840 A).

Open porosity, specific gravity and water absorption were measured according to the RILEM CPC 11.3 method [13], which included the vacuum conditioning of dried stone specimens without water and immersed in water. The water absorption coefficient by capillarity was measured using cubic stone specimens (about 50 × 50 × 50 mm), which were previously dried for 24 h at 60 °C and then immersed in 5 to 10 mm of water for 72 h, while the weight of the specimens was regularly recorded [14]. The compressive strength was measured using the MATEST compression strength machine [15].

The thermophysical parameters were measured using a KD2 Pro Thermal Properties Analyzer (Decagon Devices). Two different sensors were applied: (a) the large (10 cm long, 2.4 mm diameter) single needle TR-1 sensor, which measures thermal conductivity and thermal resistivity and is primarily designed for granular or porous materials; and (b) the dual needle SH-1 sensor, which, beyond the aforementioned properties, measures volumetric heat capacity and thermal diffusivity. Both sensors measure the thermal properties with an accuracy of 10%. Two stone samples, collected from the locations 1 and 2 (Figure 1b), were subjected to thermal properties measurements.

3. Results and Discussion

3.1. On-Site Macroscopic Observations

The on-site macroscopic examination revealed a variety of decay phenomena, such as peeling, biological colonization, disintegration, fragmentation and cracking, as shown in the photographs in Figure 3. Several portions of the stone structures exhibited local collapses and lacunas, indicating a variation of both the nature of the stone and the degree of deterioration, even between the stones that comprise a specific monument structure (Figure 3d). The absorption and stagnation of capillary water resulted in the significant swelling of the stones and, consequently, in the material degradation. The incoherent, porous and highly water absorbent stone materials allowed the formation and rooting of vegetation, resulting in further deterioration of the stone (Figure 3a,c). The existence of water in the bulk of the materials due to capillary water absorption, freeze–thaw cycles, dissolution and crystallization of salts can also result in partial dissolution–recrystallization of the carbonate material and loss of the structural cohesion and the surface stability of the stones. Water absorption, freeze–thaw cycles and biological colonization have been reported by Kouzeli (2009) [5] as the main factors contributing to the stone deterioration of the archaeological site of Pella. The exfoliation and fragmentation of the stone material were commonly observed, while the formation of long cracks, associated with the action of frost, was also recorded.

Figure 3. (**a**–**f**) The state of preservation of the building stone at the archaeological site of Pella.

Moreover, the climate conditions in the Pella area are characterized by wet periods with increased moisture and rainfall, by dry periods with insolation and by high temperature differences that significantly favor the mechanical, chemical and biological decay of the stones.

A large diversity of species colonizing the surface of the stone was also observed during the on-site macroscopic examination. Overall, 17 species of lichens were identified, including some species (e.g., *Lecanora muralis* and *Xanthoria parietina*) that display an endolithic habit, with the thallus growing entirely within the rock substrate, exploiting internal cracks or the pores of the stone [16,17]. They often grow in cracks and pores and may erode the rocks. Figure 4 shows examples of lichens colonizing the stone surface. Their colors range from white, yellow, orange, green, dark brown and dark gray to black. The observed mechanisms of the deterioration of the stones resulting from lichen growth were varied, from the formation of biofilms to discoloration, salting and physical damage to the production of osmolytes and organic acids [18]. In fact, to date, there is a lack of published studies regarding the lichens' diversity, or even the colonization mode of other plant species on the stones of the archaeological site of Pella. In an earlier study at the same site, up to 12 species of mosses were detected on stones in the area of the Palace [19]. This number of species was higher compared to other areas included in the same study, such as the archeological site of Amphipolis, where eight species were observed, Vergina with ten species and the Roman market in Thessaloniki with nine species of mosses. The high number of species detected at the archaeological site of Pella was attributed to the high percentage of humidity observed in the area compared to the other studied areas [19].

Figure 4. Examples of lichens colonizing the stone.

3.2. Petrographic, Mineralogical and Physicochemical Characteristics

Stereomicroscopy revealed discoloration, cracks and newly formed calcite crystals that were deposited in large pores and voids, which can affect the mechanical strength of the stone. The crystallization of calcite may occur when water, which carries dissolved $CaCO_3$, flows within the pores and voids of the limestone either during diagenesis or when it was used as a building material at the site and was exposed to atmospheric precipitation. Selected images taken from the stereoscopic observation of the stones are shown in Figure 5.

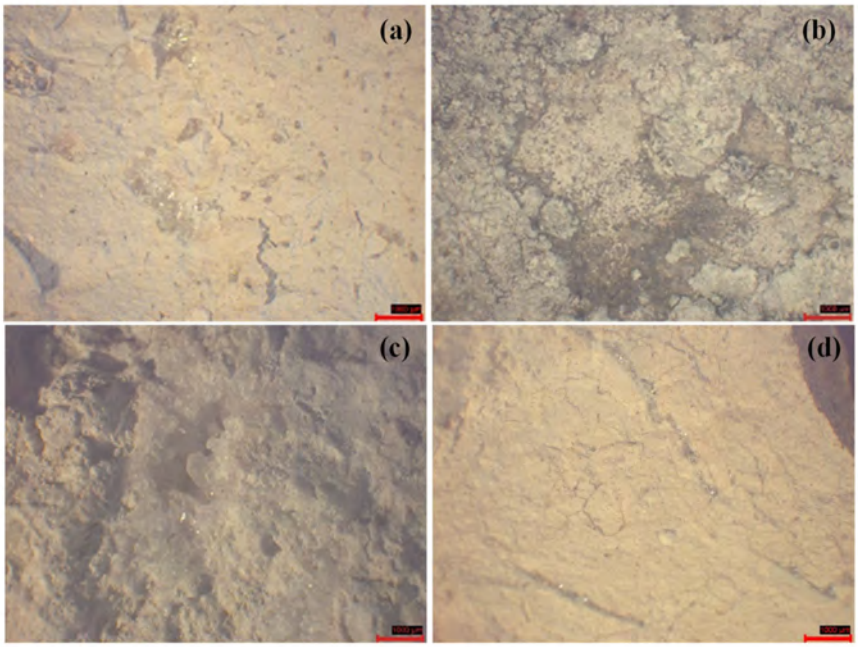

Figure 5. Microstructure of stone samples collected from sampling points 2 (**a**), 3 (**b**), 4 (**c**) and 5 (**d**).

It was shown that the samples examined consisted of marly limestone. Most samples suffered from surface alterations and material degradation, with biological deterioration commonly revealed. Exfoliation, cracks and discontinuities were observed, while stone flakes 1 mm deep were often detached from the surface, leading to material loss. Stone deterioration was also observed due to biological attack, mainly on the surface, but also at a depth of a few millimeters.

The examination of the samples revealed the lithotype, namely, a marly limestone, which is the most common rock in the broader area of Pella (Figure 1) [4] and dates to the upper Miocene age (7.3–5.3 million years ago). The Miocene character of the stone was also supported by the isotopic analysis of the stone collected from sampling location 5. The isotopic analysis gave the following results: δ18O: −7.45 ‰ and δ13C: −5.13 ‰, which are typical for limestone from the Miocene age [20]. Other lithologies around the archaeological site of Pella are marls and loose sandstones (Figure 1) that are not suitable for building purposes.

An example of the microscopic study of the samples collected from points 5 and 6 is provided in Figure 6. The mineralogical composition of the rock consists of calcite with grains of <1 μm in length (Figure 6a). The sample also comprises traces of clasts of granular quartz, microcline and calcite, as well as plates of muscovite and biotite, with a length

<150 μm (Figure 6a–c,e–f). Occasionally, microfossils occur throughout the limestone (Figure 6d). They are not always well preserved due to the subsequent diagenesis and tectonics. The marly limestone from Pella contains numerous pores, with diverse size and distribution in the rock (Figure 6e,f). These pores have a diameter up to 0.5 mm and are sometimes filled with secondary calcite crystals (Figure 6e).

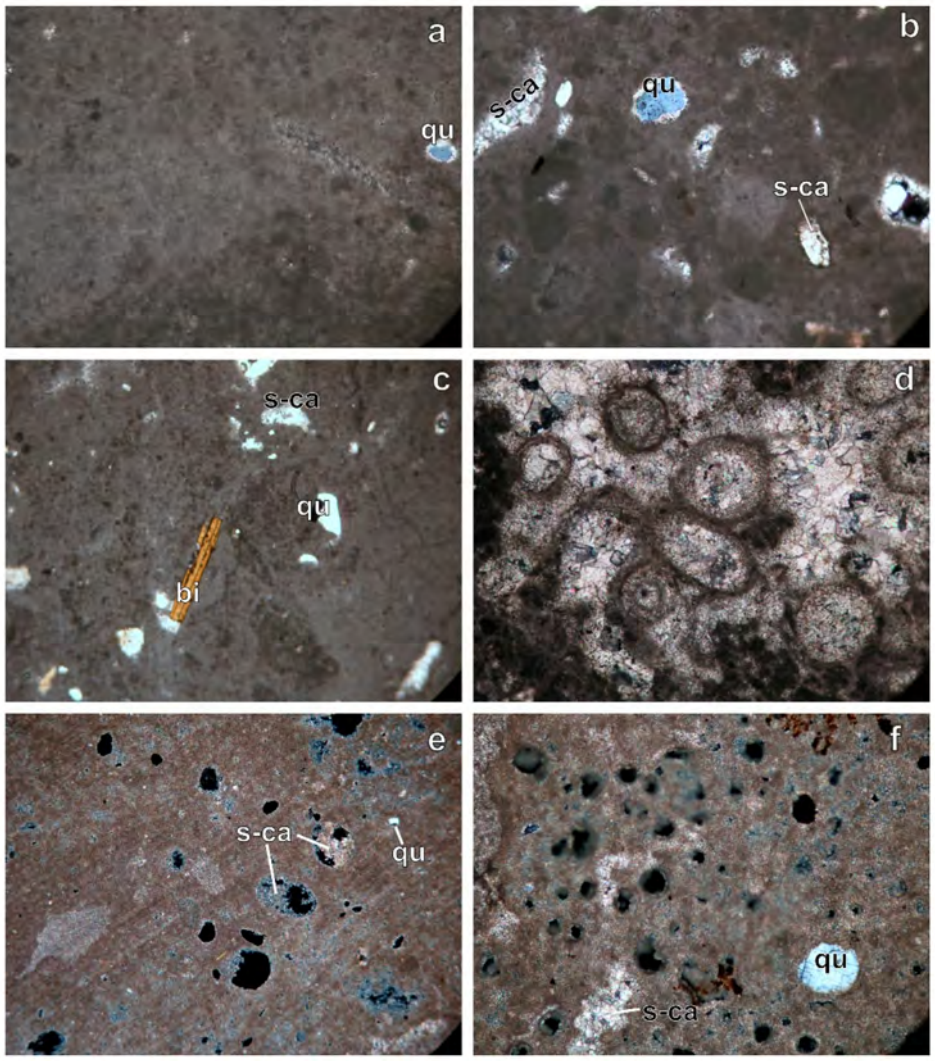

Figure 6. Thin-section micrographs of the stone sample collected from sampling points 5 and 6. Micrographs obtained from polarized microscope. (**a**). The marly limestone with calcite grains <1 μm and a clast of quartz (qu). (**b**). Quartz (qu) and calcite clasts (s-ca) in the marly carbonate material. (**c**). Quartz (qu) and calcite clasts (s-ca) and a plate of biotite (bi) in the marly material. (**d**). Ooidal microfossils made of calcite. (**e**). Pores (black spots) in the marly limestone, partly replaced by secondary calcite (s-ca). (**f**). Numerous pores (black spots) in the marly limestone, and quartz (qu) and calcite (s-ca) clasts. (**a**–**f**): +N; c://N; photography length: 750 μm.

The results obtained from the XRD analysis showed that the dominant mineral phase of the limestone is calcite, while quartz and clay minerals were also detected in traces. The XRD patterns of the stone samples collected from sampling points 2, 3, 5 and 7 are shown in Figure 7. In these patterns, it is obvious that the clay minerals are absent or are found in low concentrations. Therefore, in the case of Pella, the nature of the marly limestone is the main factor that promotes intracrystalline disintegration, formation of microcracks, increase of porosity and disruption of the internal cohesion of the stone.

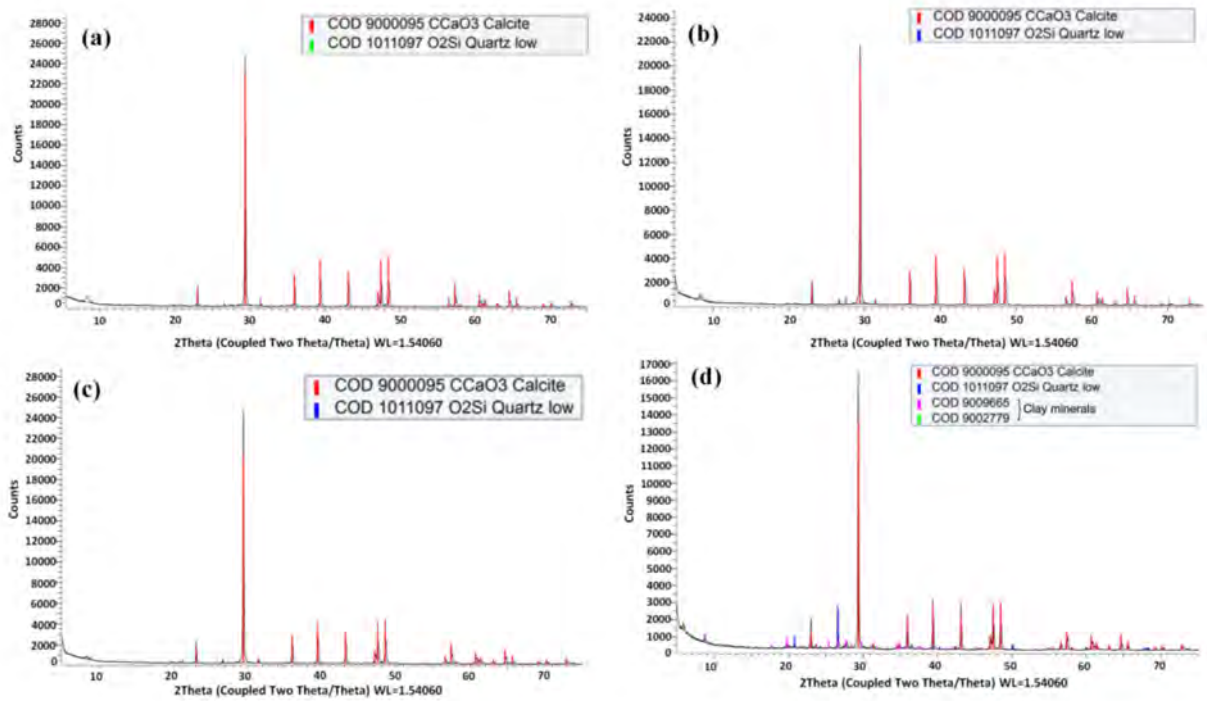

Figure 7. XRD patterns of stone samples collected from sampling point 2 (**a**), 3 (**b**), 5 (**c**) and 7 (**d**).

SEM images revealed the porous structure of the rock samples. For example, SEM images for limestone collected from sampling points 5 and 6 are provided in Figure 8, while the corresponding SEM–EDS results obtained for the areas designated in the SEM images are given in Tables 2 and 3, respectively. As can been seen from the images, a fiber structure is formed due to biological deposits (e.g., Figure 8d) and the porous surface of calcite is observed. Moreover, the mechanical disintegration of the rock is visible, as the microfossils are almost detached from the stone matrix (Figure 8c).

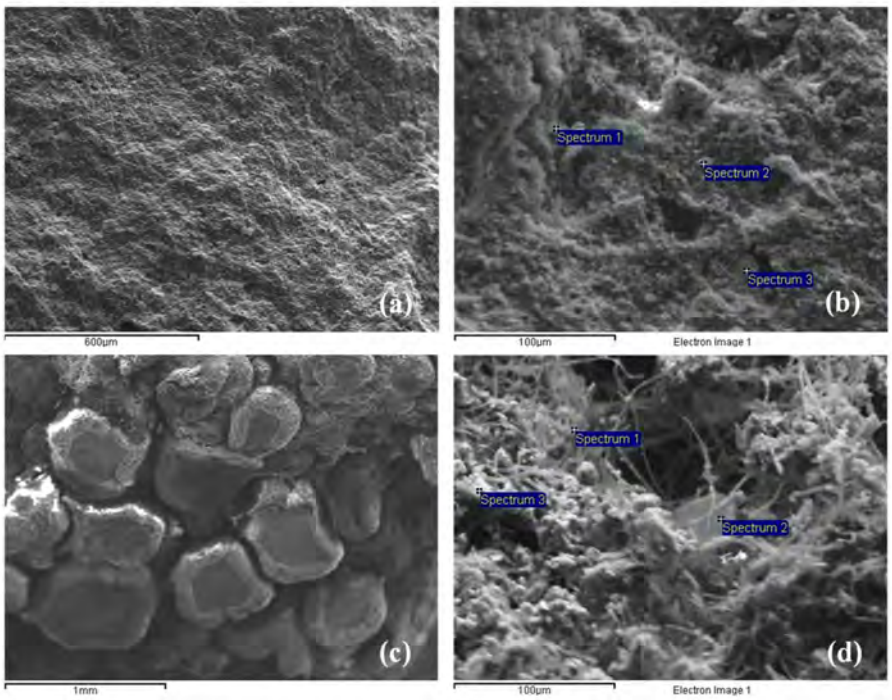

Figure 8. Examples of SEM images for stones collected from sampling points 5 (**a**) and (**b**) and 6 (**c**) and (**d**).

Table 2. SEM–EDS results for stone collected from sampling point 5 (the corresponding spectrum is shown in Figure 8b).

Spectrum	O	Mg	Al	Si	K	Ca
Spectrum 1	72.8	2.6	2.5	10.1	-	12.0
Spectrum 2	69.5	1.0	1.1	3.4	-	25.0
Spectrum 3	63.9	3.6	3.9	14.1	1.3	13.3
Mean	68.7	2.4	2.5	9.2	1.3	16.8
Std. Deviation	4.5	1.3	1.4	5.4	-	7.2

Table 3. SEM–EDS results for stone collected from sampling point 6 (the corresponding spectrum is shown in Figure 8d).

Spectrum	O	Mg	Al	Si	S	K	Ca	Fe
Spectrum 1	70.8	1.3	2.4	12.9	1.0	0.9	10.8	-
Spectrum 2	65.6	1.4	5.4	15.2	1.0	1.3	8.2	2.1
Spectrum 3	57.9	2.0	8.9	21.0	-	1.8	4.5	3.8
Mean	64.8	1.6	5.6	16.3	1.0	1.3	7.8	3.0
Std. Deviation	6.5	0.4	3.3	4.2	0.0	0.5	3.2	1.2

The results in Tables 2 and 3 show that high concentrations of O, Ca and Si were recorded. These SEM–EDS results are in agreement with the XRD data that showed that calcite and quartz were the dominant crystalline phase of the stones. The presence of aluminum, probably as aluminum silicate, is also confirmed in Tables 2 and 3, while the detection of iron (probably in the form of iron oxides) in the stone collected from sampling point 6 is indicative of the reddish color of this stone sample (Figure 2). In addition, the detection of S in the stone from sampling point 6 may be related to the infection of the stone by sulfate salt decay (gypsum) $CaSO_4 \cdot 2H_2O$ [11]. This is supported by the SEM images, which revealed a mechanical disintegration of the stone material (Figure 8c).

3.3. Physicomechanical Characteristics

Table 4 presents the results of the measurements of the porosity, specific gravity, water absorption coefficient and compressive strength of the stone samples collected from the seven sampling points. For most samples, the porosity values ranged between 12.06 and 21.09%. For these samples, the specific gravity ranged from 2.03 to 2.07, whereas water absorption was between 9.22 and 10.40%. However, for the stone collected from sampling point 4, the corresponding values were quite different. In particular, porosity was 12.06%, specific gravity 2.28 and water absorption 5.30%. Finally, the compressive strength was low and ranged from 11.27 to 27.73 MPa.

Table 4. Physicomechanical characteristics of stone samples collected from the seven sampling points.

Parameter	Mean Value *	Min	Max
Porosity (%)	18.4 ± 3.6	12.06	21.09
Specific gravity	2.1 ± 0.1	2.03	2.28
Water absorption (%)	8.8 ± 2.0	5.3	10.4
Water absorption coefficient ($g/m^2 \cdot s^{0.5}$)	27.2 ± 6.8	15.9	35.4
Compressive strength (MPa)	19.1 ± 7.8	11.3	27.7

* Mean values and standard deviation were calculated based on the measurement of at least five stone samples.

For all samples, the specific gravity values were within the range of values usually reported for limestones [11,21]. The water absorption coefficient varied from 15.9 to 35.4 g/m^2·s$^{0.5}$, while water absorption from 5.3 to 10.4%. Lower values of water absorption for porous stone materials were reported by Avdelidis et al. [22]. The porosity values reported in Table 4 are somewhat higher compared to previously published results [21]. In particular, it was reported that the porosity of samples characterized as heavily deteriorated varied between 9.0 and 11.0%, while those characterized as healthy samples were between 1.5 and 3.5% [21]. In the same study, the corresponding values for absorption were between 2.50 and 4.85% and 0.64 and 1.50% for samples characterized as heavily deteriorated and healthy samples, respectively. Furthermore, it was found that the porosity of unweathered limestone samples collected from a nearby quarry varied between 1.38 and 9.40%, with a compressive strength between 20 and 45 MPa [3]. Overall, higher porosity and lower compressive strength values were recorded in our study, indicating a different stone nature or the potential deterioration of the stone at the archaeological site.

3.4. Thermographical Characteristics

Figure 9 presents thermal conductivity (K) measurements as a function of read time, employing both KD2 Pro sensors, for stones collected from sampling points 1 and 2. Each point displays the average K value resulting from nine measurements (three repetitions for three different measuring points). The respective error bars have also been added to the data points. For both samples, the K values resulting from the different sensors are in fair agreement. In addition, the K increases with read time. The measurements for a 10 min read time are considered more reliable due to minimized error. The K value of the stone collected from sampling point 2 is higher than that of sampling point 1:1.85 W/m·K versus 1.58 W/m·K for a 10 min read time. Such variation is expected. Even rocks from the same area differ in density, porosity and water absorption and this can influence the thermal conductivity considerably. Canakci et al. [23] developed some empirical equations that correlate the measured K with the density (δ, kg/m^3), porosity (p, -) and water absorption (w, %) of dried limestones from Gaziantep (Turkey), as shown below:

$$K = 0.0861e^{0.0014\delta} \quad (1)$$

$$K = 3.0907e^{-2.4195p} \quad (2)$$

$$K = 3.2767e^{-0.0643w} \quad (3)$$

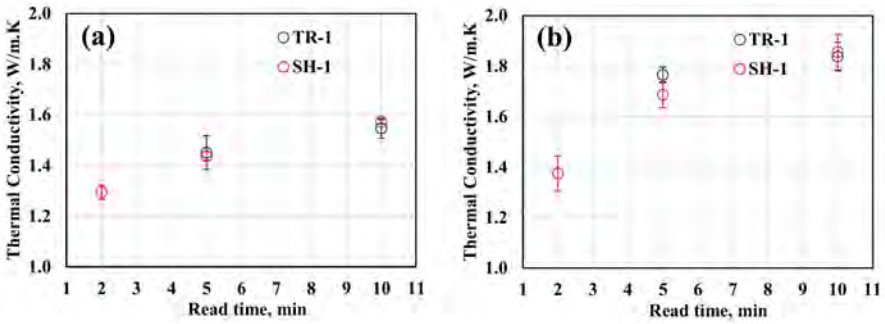

Figure 9. Measured thermal conductivity as a function of read time employing the TR-1 and SH-1 sensors of the KD2 Pro device for stones collected from sampling points 1 (**a**) and 2 (**b**).

Equations (1)–(3) are applied to predict the K values based on the measured δ, p and w values of our limestones. Thus, K ranges from 1.42 W/m·K to 1.88 W/m·K for δ ranging from 2000 to 2200 kg/m^3; from 2.16 W/m·K to 1.81 W/m·K for p ranging from 0.14 to 0.22; and from 2.12 W/m·K to 1.63 W/m·K for w ranging from 7% to 11%. In conclusion, the calculated K values range from ~1.4 W/m·K to ~2.2 W/m·K and, consequently, the K measurements shown in Figure 7 are considered realistic.

Furthermore, Figure 10 shows the thermal diffusivity (D) and specific heat capacity (c_p) measurements for the stone collected from sampling point 1. The c_p values were calculated from the measured volumetric specific heat values (SH-1 sensor) and measured average density (2100 kg/m^3). Although D increases with read time, c_p remains almost constant when the read time increases from 2 min to 10 min. The D value for a 10 min read time, ~0.9 mm^2/s, approaches the lower D values measured by Merriman et al. [24], 0.8 mm^2/s to 1.6 mm^2/s, while the corresponding c_p value of ~0.9 KJ/kg· K is in fair agreement with the literature value of 0.91 KJ/kg· K [25].

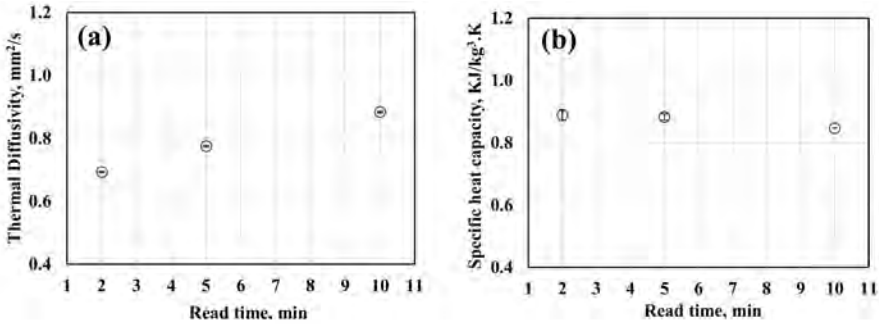

Figure 10. Thermal diffusivity (**a**) and specific heat capacity (**b**) as a function of read time for stone collected from sampling point 1, measured using the SH-1 sensor of the KD2 Pro device.

The measured values of thermal conductivity, thermal diffusivity and specific heat capacity for two samples are presented in Tables 5 and 6.

Table 5. Measured thermal conductivity for varying read time, employing TR-1 and SH-1 sensors of the KD2 Pro device for stone samples.

Read Time, min	Thermal Conductivity, W/m·K			
	Stone from Sampling Point 1		Stone from Sampling Point 2	
	Sensor TR-1	Sensor SH-1	Sensor TR-1	Sensor SH-1
2	-	1.294 ± 0.028	-	1.375 ± 0.069
5	1.451 ± 0.067	1.437 ± 0.016	1.766 ± 0.031	1.687 ± 0.052
10	1.547 ± 0.040	1.572 ± 0.007	1.838 ± 0.057	1.856 ± 0.071

Table 6. Thermal diffusivity and specific heat capacity for varying read time, as measured using the SH-1 sensor of the KD2 Pro device.

Read Time, min	Stone from Sampling Point 1/Sensor SH-1	
	Thermal Diffusivity, mm^2/s	Specific Heat Capacity, KJ/kg^3·K
2	0.694 ± 0.002	0.888 ± 0.017
5	0.775 ± 0.003	0.883 ± 0.009
10	0.884 ± 0.003	0.847 ± 0.000

The determination of the limestone samples' thermophysical properties is critical, because the thermal performance of the material affects its decay across time. Therefore, the obtained data can contribute towards the assessment of limestone characteristics when combined with other measured parameters in this study. Interestingly, Canaksi et al. [23] found an exponential relationship between the water absorption and thermal conductivity of the limestone samples, while Currulli et al. [12] suggested the application of thermographical techniques for the evaluation of the hydraulicity degree of mortar samples. The measured thermal conductivity values are within the range of values found in the literature, while the specific heat capacity value is in fair agreement with the literature. With

regard to the measured value of thermal diffusivity, it is close to the lower values found in the literature. Since thermal diffusivity is the measure of thermal inertia, such a low value indicates that heat moves relatively slowly through the material. Consequently, the decay of the limestone due to ambient temperature variation and the corresponding contraction/expansion phenomena is relatively limited. This information will be taken into consideration for the selection of proper coating materials.

4. Conclusions

The assessment of the characteristics of stone building materials is a relatively difficult task, as the stone, which is exposed to atmospheric conditions, is subjected to various physicochemical and biochemical alterations. These alterations may vary significantly in an archaeological site, resulting in various decay mechanisms of the stone and, consequently, to its various degrees of deterioration. Therefore, the application of a wide variety of analytical techniques for the evaluation of the mineralogical, chemical, mechanical and thermal properties of the stone can be very useful for an overall characterization of the stone and the evaluation of its degree of deterioration. The overall results of this study have shown that the state of preservation of the natural stone at the archaeological site of Pella may be characterized as extremely poor.

Several portions of the stone structures exhibited local collapses, implying a variation of both the nature of the stone and the degree of deterioration, even between the stones that comprise a specific monument structure. Water absorption and biological colonization were the main factors resulting in the deterioration of the stone. The microscopic examination of the samples showed that the main natural stone at the archaeological site is a marly limestone. The main lithologies around the archaeological site of Pella are marly limestones, marls and loose sandstones. Consequently, marly limestones were the only suitable local rocks for building structures in the nearby area, with a small transporting distance.

Most of the samples examined indicated surface alterations and material degradation, along with biological deterioration. The mineralogical examination showed that the main mineral of the investigated limestone is calcite, with minor quartz and traces of microcline, muscovite and biotite. Clay minerals are absent or are found in traces, too. This shows that the main factor that controls the disintegration of the building stones is the nature of the marly limestone, and not the clay phases themselves, which are detected in low concentrations.

The high porosity values detected in almost all of the studied samples, as well as the relatively low compressive strength, reveal the vulnerability of the stone at the archaeological site and the need to take conservation measures. The thermographical measurements showed that the ambient temperature variation may not contribute extensively to the decay phenomena, as a relatively low thermal diffusivity was recorded for the studied stones. In sum, an efficient conservation and restoration scheme should combine all of the information collected from the petrographic, physicochemical, physicomechanical and thermographical characterization of the stone.

Author Contributions: Conceptualization, P.K.S., I.K. and T.D.K.; methodology, I.K., V.M.; formal analysis, E.G., S.P.E. and V.M.; investigation, M.M., E.G. and V.M.; data curation, M.M., E.G. and V.T.; writing—original draft preparation, M.M., V.T. and S.P.E., writing—review and editing, V.T., S.P.E., I.K. and V.M.; visualization, V.T., S.P.E., I.K. and V.M.; supervision, P.K.S. and T.D.K.; project administration, P.K.S. and T.D.K.; funding acquisition, P.K.S. and T.D.K. All authors have read and agreed to the published version of the manuscript.

Funding: This research was funded by EPAnEK—ESPA 2014–2020 Special Actions "Aquaculture—Industrial Materials—Open Innovation in Culture" (Program code: T6ΥΒΠ-00069).

Institutional Review Board Statement: Not applicable.

Informed Consent Statement: Not applicable.

Acknowledgments: This study was carried under the program 'Diagnostic and Preservation Open Lab of the buildings and the Palace of Pella' funded by EPAnEK—ESPA 2014–2020 Special Actions "Aquaculture—Industrial Materials—Open Innovation in Culture" (Program code: Τ6ΥΒΠ-00069). The authors would like to thank E. Tsigarida and V. Chrysostomou (Ephorate of Antiquities of Pella), and M. Stefanidou, L. Papadopoulou, E. Pavlidou and T. Savvidis (Aristotle University of Thessaloniki).

Conflicts of Interest: The authors declare no conflict of interest.

References

1. Spathis, P.; Papanikolaou, E.; Melfos, V.; Samara, C.; Christaras, B.; Katsiotis, N. Characterization and Weathering of the Building Materials of Sanctuaries in the Archaeological Site of Dion, Greece. *Trends J. Sci. Res.* **2015**, *2*, 95–103.
2. Liali, T.; Chrysostomou, E.; Karasarlidis, E. *Maintenance and Restoration Study of the Propylon and the Building I of the Palace of Pella*; Ephorate of Antiquities of Pella: Pella, Greece, 2018. (In Greek)
3. Papayianni, I.; Stefanidou, M.; Pachta, V. *Survey of Repaired and Artificial Stones of the Archaeological Site of Pella Five Years after Application*; Springer: Singapore, 2014; pp. 431–442.
4. Xydas, S.; Efstratides, G. *Geological Map of Greece, Koufalia Sheet, 1:50,000*; IGME: Athens, Greece, 1993.
5. Kouzeli, K. *Stone of the Archaeological Site of Pella—Special Features—Decay Mechanism—Conservation Proposals*; Ministry of Culture, Stone Center: Athens, Greek, 2009. (In Greek)
6. Grossi, C.M.; Brimblecombe, P.; Harris, I. Predicting long term freeze–thaw risks on Europe built heritage and archaeological sites in a changing climate. *Sci. Total Environ.* **2007**, *377*, 273–281. [CrossRef] [PubMed]
7. Thomas, C.; Lombillo, I.; Setién, J.; Polanco, J.A.; Villegas, L. Characterization of materials with repellents and consolidants from a historic building. *J. Mater. Civil Eng.* **2013**, *25*, 1742–1751. [CrossRef]
8. Herrera, L.K.; Videla, H.A. Surface analysis and materials characterization for the study of biodeterioration and weathering effects on cultural property. *Int. Biodeterior. Biodegrad.* **2009**, *63*, 813–822. [CrossRef]
9. Ruedrich, J.; Kirchner, D.; Siegesmund, S. Physical weathering of building stones induced by freeze–thaw action: A laboratory long-term study. *Environ. Earth Sci.* **2010**, *63*, 1573–1586. [CrossRef]
10. Török, Á. Surface strength and mineralogy of weathering crusts on limestone buildings in Budapest. *Build. Environ.* **2003**, *38*, 1185–1192. [CrossRef]
11. Amer, O.; Aita, D.; Mohamed, E.K.; Torky, A.; Shawky, A. Experimental Investigations and Microstructural Characterization of Construction Materials of Historic Multi-Leaf Stone-Masonry Walls. *Heritage* **2021**, *4*, 135. [CrossRef]
12. Curulli, A.; Montesperelli, G.; Ronca, S.; Cavalagli, N.; Ubertini, F.; Padeletti, G.; Ciprioti, S.V. A multidisciplinary approach to the mortars characterization from the Town Walls of Gubbio (Perugia, Italy). *J. Therm. Anal. Calorim.* **2020**, *142*, 1721–1737. [CrossRef]
13. Recommendations, R. Absorption of water by immersion under vacuum. *Mater. Struct.* **1984**, *101*, 391–394.
14. European Committee for Standardization. *Natural Stone Test Methods—Determination of Water Absorption Coefficient by Capillarity*; EN 1925; European Committee for Standardization: Brussels, Belgium, 1999.
15. European Committee for Standardization. *Natural Stone Test Methods—Determination of Uniaxial Compressive Strength*; EN 1926; European Committee for Standardization: Brussels, Belgium, 2006.
16. Dakal, T.C.; Cameotra, S.S. Microbially induced deterioration of architectural heritages: Routes and mechanisms involved. *Environ. Sci. Eur.* **2012**, *24*, 36. [CrossRef]
17. Pinna, D.; Salvadori, O.; Tretiach, M. An anatomical investigation of calcicolous endolithic lichens from the Trieste karst (NE Italy). *Plant Biosyst.-Int. J. Deal. All Asp. Plant Biol.* **1998**, *132*, 183–195. [CrossRef]
18. Scheerer, S.; Ortega-Morales, O.; Gaylarde, C. Microbial deterioration of stone monuments –An updated overview. *Adv. Appl. Microbiol.* **2009**, *66*, 97–139. [PubMed]
19. Papakosta, V. Colonization with Mosses of Archaeological Sites and Monuments. Master's Thesis, Aristotle University of Thessaloniki, Thessaloniki, Greek, 2012. (In Greek).
20. Dotsika, E.; Psomiadis, D.; Poutoukis, D.; Raco, B.; Gamaletsos, P. Isotopic analysis for degradation diagnosis of calcite matrix in mortar. *Anal. Bioanal. Chem.* **2009**, *395*, 2227–2234. [CrossRef] [PubMed]
21. Stefanidou, M.; Pachta, V.; Papayianni, I. Design and testing of artificial stone for the restoration of stone elements in monuments and historic buildings. *Constr. Build. Mater.* **2015**, *93*, 957–965. [CrossRef]
22. Avdelidis, N.; Moropoulou, A.; Theoulakis, P. Detection of water deposits and movement in porous materials by infrared imaging. *Infrared Phys. Technol.* **2003**, *44*, 183–190. [CrossRef]
23. Çanakci, H.; Demirboğa, R.; Karakoç, M.B.; Şirin, O. Thermal conductivity of limestone from Gaziantep (Turkey). *Build. Environ.* **2007**, *42*, 1777–1782. [CrossRef]
24. Merriman, J.D.; Hofmeister, A.M.; Roy, D.J.; Whittington, A.G. Temperature-dependent thermal transport properties of carbonate minerals and rocks. *Geosphere* **2018**, *14*, 1961–1987. [CrossRef]
25. Engineering ToolBox, Specific Heat of Solids. 2003. Available online: https://www.engineeringtoolbox.com/specific-heat-solids-d_154.html (accessed on 27 May 2021).